Renewable and Sustainable Energy Reviews 15 (2011) 1545–1555

Contents lists available at ScienceDirect

Renewable and Sustainable Energy Reviews

journal homepage: www.elsevier.com/locate/rser

Evaluation of NWP performance for wind energy resource assessment in Oman

Yassine Charabi[a,*], Sultan Al-Yahyai[b], Adel Gastli[b]

[a] Department of Geography, College of Arts and Social Sciences, Sultan Qaboos University, P.O. 42, Al-Khodh, Muscat-123, Oman
[b] Department of Electrical & Computer Engineering, College of Engineering, Sultan Qaboos University, P.O. 33, Al-Khodh, Muscat-123, Oman

ARTICLE INFO

Article history:
Received 1 June 2010
Accepted 24 November 2010
Available online 12 January 2011

Keywords:
Assessment
NWP
Oman
Satellite data
Wind energy

ABSTRACT

Few studies have been conducted to evaluate the wind energy potential in Oman. All of the published studies were based on ground measurements from weather stations, which provide wind data at 10 m above the ground. The spatial and temporal coverage of the actual meteorological network in Oman presents some inadequacy with the need of the wind power industry in term of data sets. Currently, these assessments are done on a site-by-site basis, using existing station data and limited on-site monitoring data. A primary task under this research is to supplement existing wind-power potential assessments and develop an enhanced (spatially explicit) inventory of the wind resource across Oman. With the current available computational power, it is possible to use of high resolution numerical weather prediction (NWP) models to provide wind data usable for wind energy resource assessment.

This paper evaluates the performance of NWP model data for wind energy application for Oman with a comparison to satellite data. Two models namely HRM and COSMO were used in this study. Suitable model resolution was first selected by evaluating the ability of the models to simulate weak local wind circulation (i.e. sea breeze), then one year of data was generated and compared to satellite data and ground measurements. The NWP data showed better accuracy over satellite data with comparison to the ground measurements. Wind power output was also calculated for selected sites with high potential.

Contents

1. Introduction

The threat from the Global warming and the continuously decline of the fossil fuel resources are driving the greatest shift in energy supply in the history of human civilization. As a result, renewable resources such as solar and wind energy are making constantly greater contributions to electricity production worldwide. The Sultanate of Oman is blessed with substantial solar energy resources due to its latitude and vast bare land [1–3]. However, the exploitation of this huge solar energy potential, should overcome a lot of challenges and barriers related to the climate, technologies and investments. The wind regime in Oman coupled with an extensive coastline and vast unpopulated areas have the potential to contribute significantly to the future electricity supply of the country. However, wind energy is not quite as simple to implement as some other energy sources.

Unlike a diesel power station, for example, where power only stops being produced when the diesel fuel runs out, or there is maintenance, wind energy from farm stops if the wind is too strong, not strong enough or there is an abrupt changes in wind direction. The wind variability and the non-storable character of wind energy constitute the major constraints for power system operation – how to prevent fluctuations in the power production of a wind farm from affecting the continuity of electricity supply to the consumer is a major challenge [4].

* Corresponding author.
E-mail addresses: yassine@squ.edu.om (Y. Charabi), s.alyahyai@gmail.com (S. Al-Yahyai), gastli@squ.edu.om (A. Gastli).

1364-0321/$ – see front matter
doi:10.1016/j.rser.2010.11.055

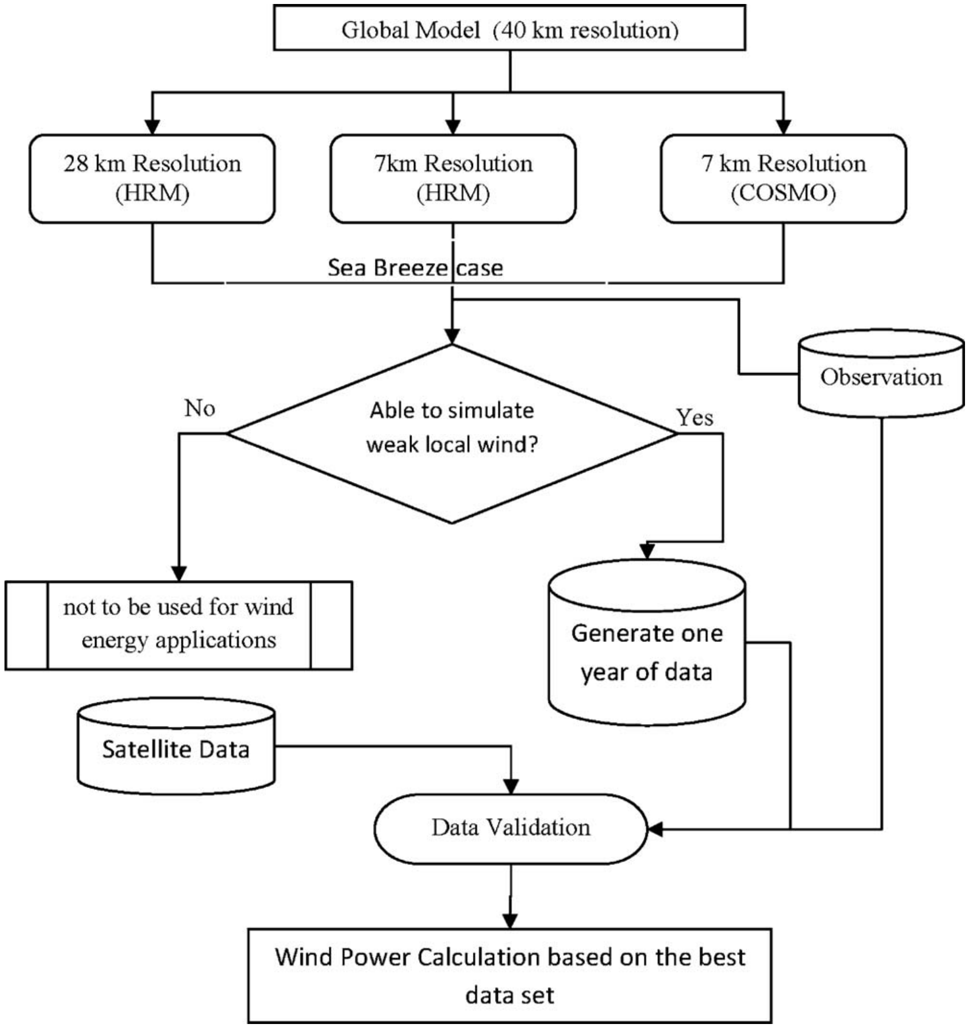


Fig. 1. Data flow diagram of the applied approach.

Climate variability and energy consumption are strongly linked. For wind power applications, variations in weather and climate play a fundamental role in determining both short-term power production from a wind plant and accurate site assessments for long-term electricity generation. Thus, the robustness and the representativeness of existing climate data sets for identifying past, current, and future trends, and variability in the potential wind resource are primordial to the ability of any country to realize their target of producing electricity from wind power [5].

Recent work reviewed published work about wind resources assessment in Oman [6]. This work involved a comparison between different studies using different data sets. It point out how the temporal resolution (hourly, daily and monthly) of the climate data sets affects resource assessment and power production estimation in Oman. The national meteorological network is probably the most relevant sources of long-term data base in Oman, but its spatial coverage and terrain representativeness is dedicated by civilian requirements; hence, most stations are located in accessible terrain. Additionally, the distribution of the available meteorological stations has very coarse resolution. As a result, the spatial and temporal coverage of the actual meteorological network in Oman presents some inadequacy with the need of the wind power industry in term of data sets. Much of these data are ground measurements (i.e. at 10 m for wind data), and they are not directly pertinent to determining the wind energy resources at typical turbine hub heights.

Precise approximations of the local wind resource and effects upon turbine performance are dependent upon atmospheric and land-surface forcings across a wide range of temporal and spatial scales – from the synoptic (thousands of km^2), through the mesoscale (tens to hundreds of km^2), down to local (km^2 or less). Thus, a comprehensive understanding of how this energy flow has an effect on resource assessment and estimated wind power production is crucial. In this regard, numerical weather predictions (NWP) models constitute key resources in such investigations. Such models are essential components of efforts to consistently simulate wind and energy resources at different spatial and temporal scales (Pryor et al. [7]).

Research undertaken to date implies regional climate simulations of wind regimes, which are strongly dependent on the general circulation models (GCM) used to provide lateral boundary conditions for regional climate model (RCM) [8]. But such comprehensive studies have not been conducted for Oman. This paper investigates the ability of NWP models to simulate local wind circulations over Oman in order to facilitate modeling for wind resource assessment purposes. Fig. 1 summarizes the approach of the study. Two different NWP models namely high resolution model (HRM) and the consortium for small-scale modeling (COSMO) model were used with 28 and 7 km resolution. German global model (GME) was used to provide the initial and lateral boundary conditions. To increase confidence in NWP wind resource estimation, the NWP outputs are compared with NASA satellite data

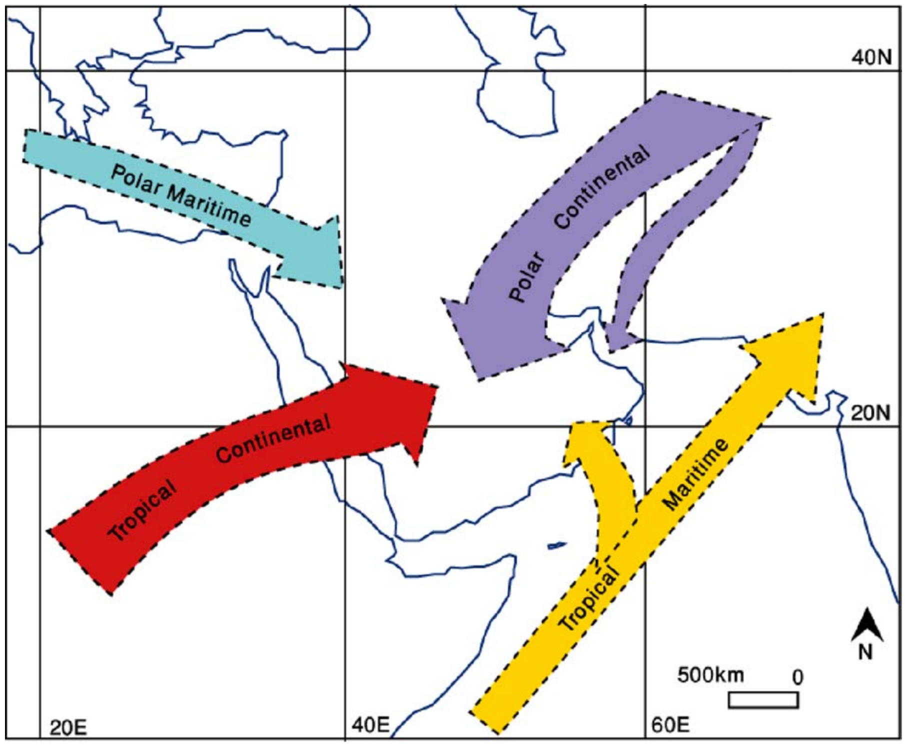


Fig. 2. Air-flow phenomena over Oman.

and ground measurement Observation taken from three weather stations.

2. Data and methodology

By virtue of its position astride the Tropic of Cancer, the Sultanate of Oman is influenced by air masses from four different directions, the Mediterranean, central Asia, the tropical maritime regime of the Indian Ocean and tropical Africa (Fig. 2). These four atmospheric mechanisms operate at different times of the year, and allow the occurrence of the two main wind regimes at synoptic scale. During winter season (December–February) Oman is dominated by a ridge of high pressure extending from the Siberian anticyclone over Asia [9]. The predominant air-flow around this system is from the northeast (we called it winter northeast monsoon). Southwest monsoon (locally known as Khareef) is characterized by winds blowing from the south-west over the Arabian Sea. It starts over the southern part of Oman from the last week of June and ends around mid September. The Arabian summer monsoon is related to the development of a succession of thermal lows across the region, with centers over northwestern India, Pakistan, Baluchistan and the Rub' al Khali [10].

Meso-scale wind circulation is also an important compound of the wind regime in Oman. It prevails along the shoreline of Oman during the weakness of the above synoptic winds and contributing significantly to ensure sustainable wind circulation all over the year. Coastal wind circulation is a meso-scale circulation that results from the differential heating between land and sea. During the day, land heats faster than the sea because it has a lower heat capacity than water. This heating causes air to rise over land. Air over the sea then rushes in horizontally to replace the rising air over land. At some level aloft, about 1 km, rising air starts to diverge and sinks over the sea forming the return flow as shown in Fig. 3. This localized air movement is called a sea breeze circulation. At night, the situation reverses as land cools faster than water and a circulation in the opposite direction develops forming a land breeze circulation.

In the tropics, the sea breeze may penetrate inland as far as 300 km, while in the mid-latitudes the inland penetration ranges between 20 and 50 km. This is due to the fact that the amount of solar radiation received in the tropics is greater than the mid-latitudes, causing a greater temperature difference needed to trigger the circulation. The strength of the sea breeze is usually proportional to the temperature difference between land and sea: the greater the temperature difference, the stronger the sea breeze. Moreover, the Coriolis force plays an important role in the sea breeze inland penetration. At the equator, the Coriolis force is zero and the sea breeze flows undeflected from sea to land. However, the Coriolis force increases with increasing latitude and

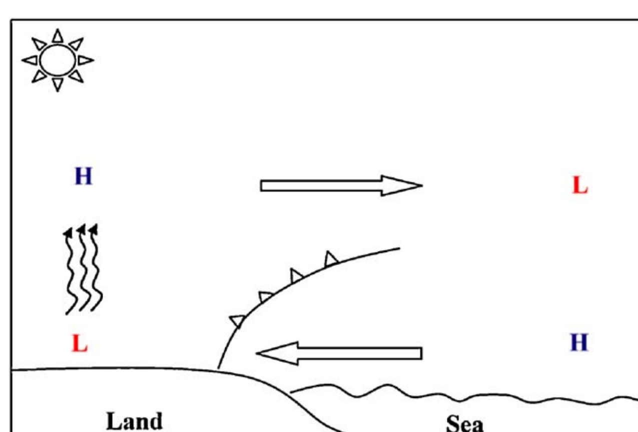


Fig. 3. Explanation of sea breeze circulations.

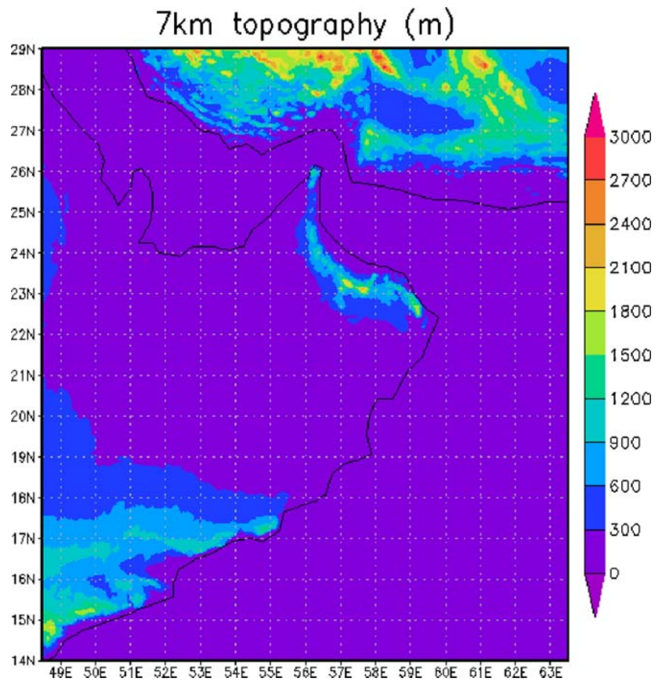


Fig. 4. Study area generated by COSMO-7.

the wind deflection increases consequently leading to less inland penetration.

A case study was conducted on the area confined between 14°E and 29°E latitude and 48.5°N and 63.5°N longitude as shown in Fig. 4. In particular, it was of interest to study the inland penetration of the sea breeze along the northern coast of Oman as well as the coast of the United Arab Emirates (UAE). The east southern coast of Oman is affected by the summer monsoon during the period between June and September; therefore it was also

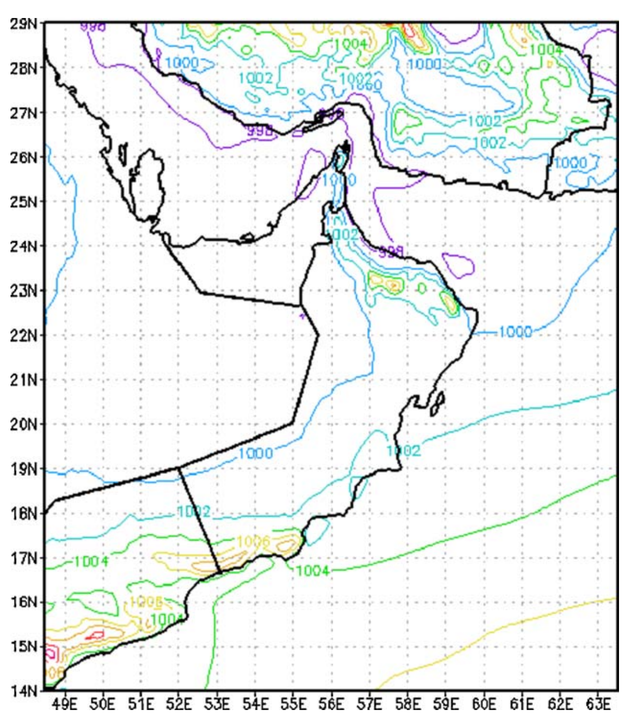


Fig. 5. Surface analysis chart based on HRM of 7 km resolution.

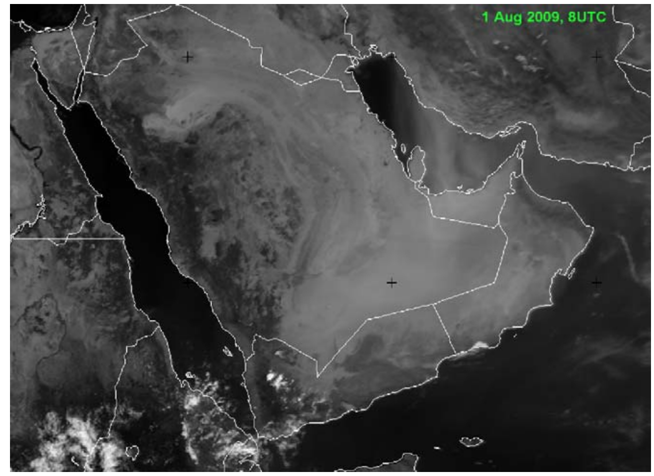


Fig. 6. Infrared channel satellite images over Oman at 8 UTC hPa.

intended to test the ability of the NWP models to simulate the summer monsoonal flow. Typical summer day (1st August 2009) was simulated and verified by surface observations. As shown in Fig. 4, the northern coast of Oman is surrounded by the chain of Al-Hajir mountains with land elevations ranging from 800 m to 2200 m in the grid of 7 km of the 7 km model. In contrast, the land surrounding the UAE coast is flat with less than 200 m land elevation.

Because of the computational power limitation, global NWP models cannot run at high resolution. Most of the operational global models run at 30–50 km resolution. However, it is rather difficult for global models to forecast local features such as sea breeze with this kind of resolution. Therefore, the need arises for a high resolution model that can recognize such meso-scale local features. Two meso-scale NWP models were used during this case study:

- High resolution model: this is a hydrostatic limited-area numerical weather prediction model for meso-α and meso-β [11,12]. Main prognostic variables are: surface pressure (p_s), temperature (T), water vapour (q_v), cloud water (q_c), cloud ice (q_i), ozone (optional), horizontal wind (u, v) and several surface/soil parameters. HRM version 2.7 was used during this simulation.

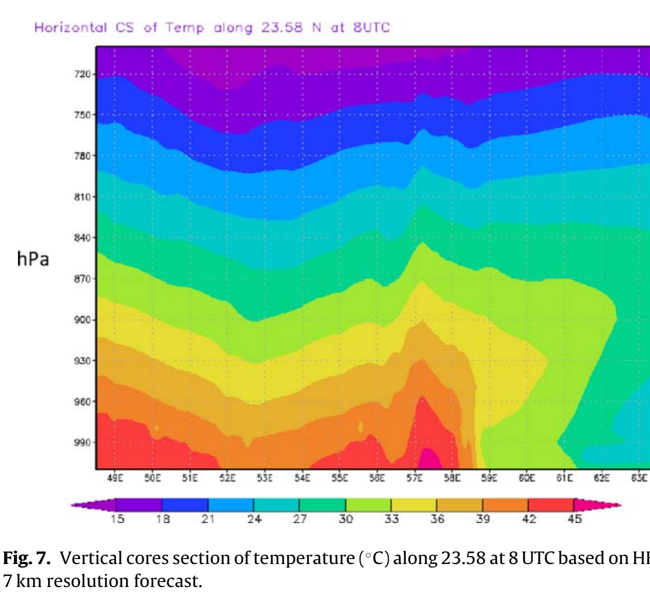


Fig. 7. Vertical cores section of temperature (°C) along 23.58 at 8 UTC based on HRM 7 km resolution forecast.

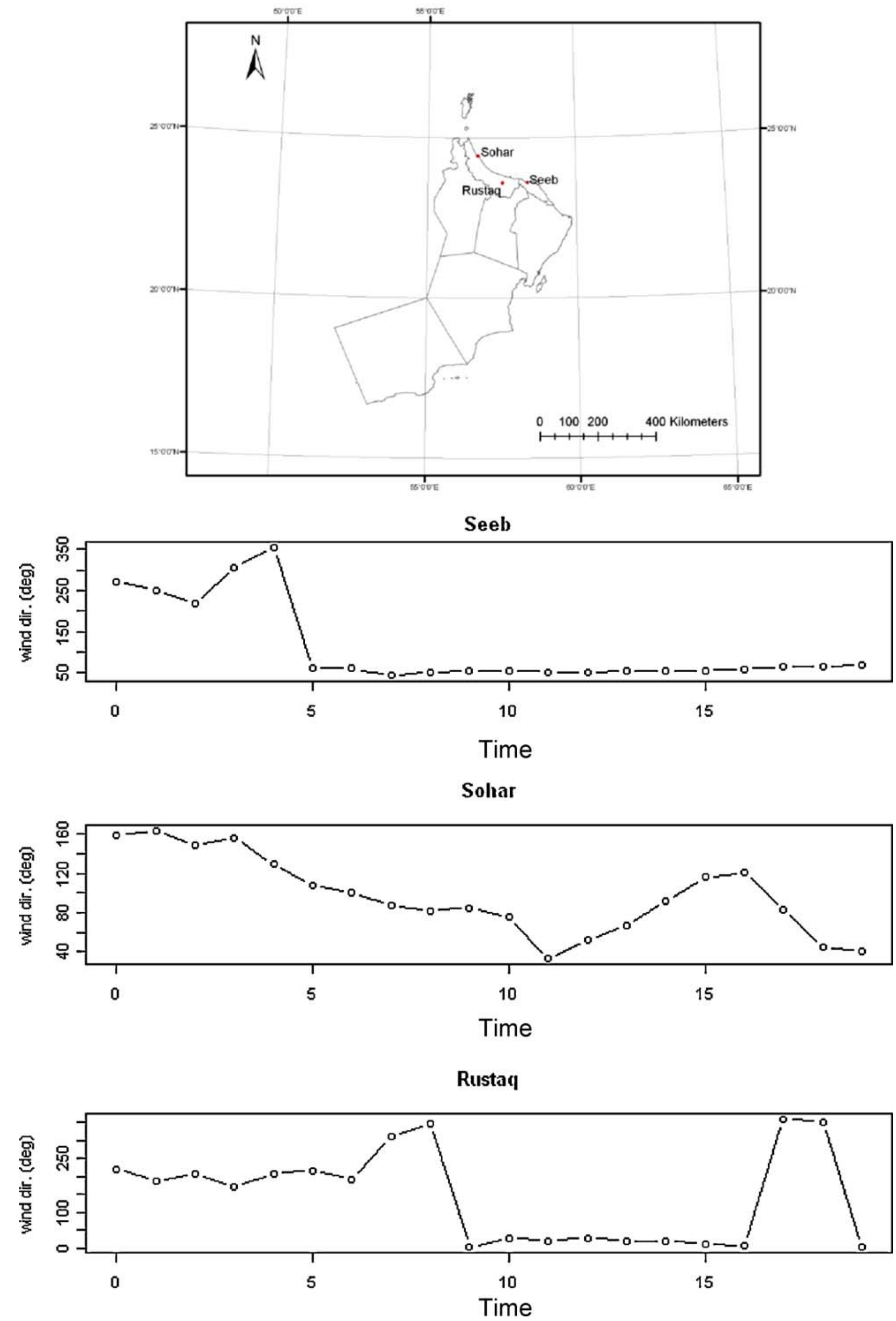


Fig. 8. Wind direction for the selected three stations: Seeb, Sohar and Rustaq.

- Consortium for small-scale modeling [11]: this is a non-hydrostatic limited-area numerical weather prediction model for meso-α and meso-β. Main prognostic variables are: pressure perturbation (p'), temperature (T), specific humidity (q_v), cloud water (q_c), cloud ice (q_i), horizontal/vertical wind (u, v) and several surface/soil parameters. COSMO version 4.3 was used during this simulation.

The performance of NWP outputs are compared with observations from ground measurements from selected site in Oman and Remote sensing information based on 10 years monthly average from NASA satellite database through http://eosweb.larc.nasa.gov/sse/. Satellite data has 1° (∼111.11 km) resolution.

3. Synopsis of the case study on the 1st of August 2009

Beside the synoptic-scale monsoonal flow, satellite images and surface maps for the beginning and the end of the 24-h analysis period shows that no synoptic-scale pressure gradients influenced the flow over the northern coast of Oman as shown in Figs. 5 and 6. As for the meso-scale effect, local topography had quite an impact on the meteorological conditions on the coastal stations. Due to

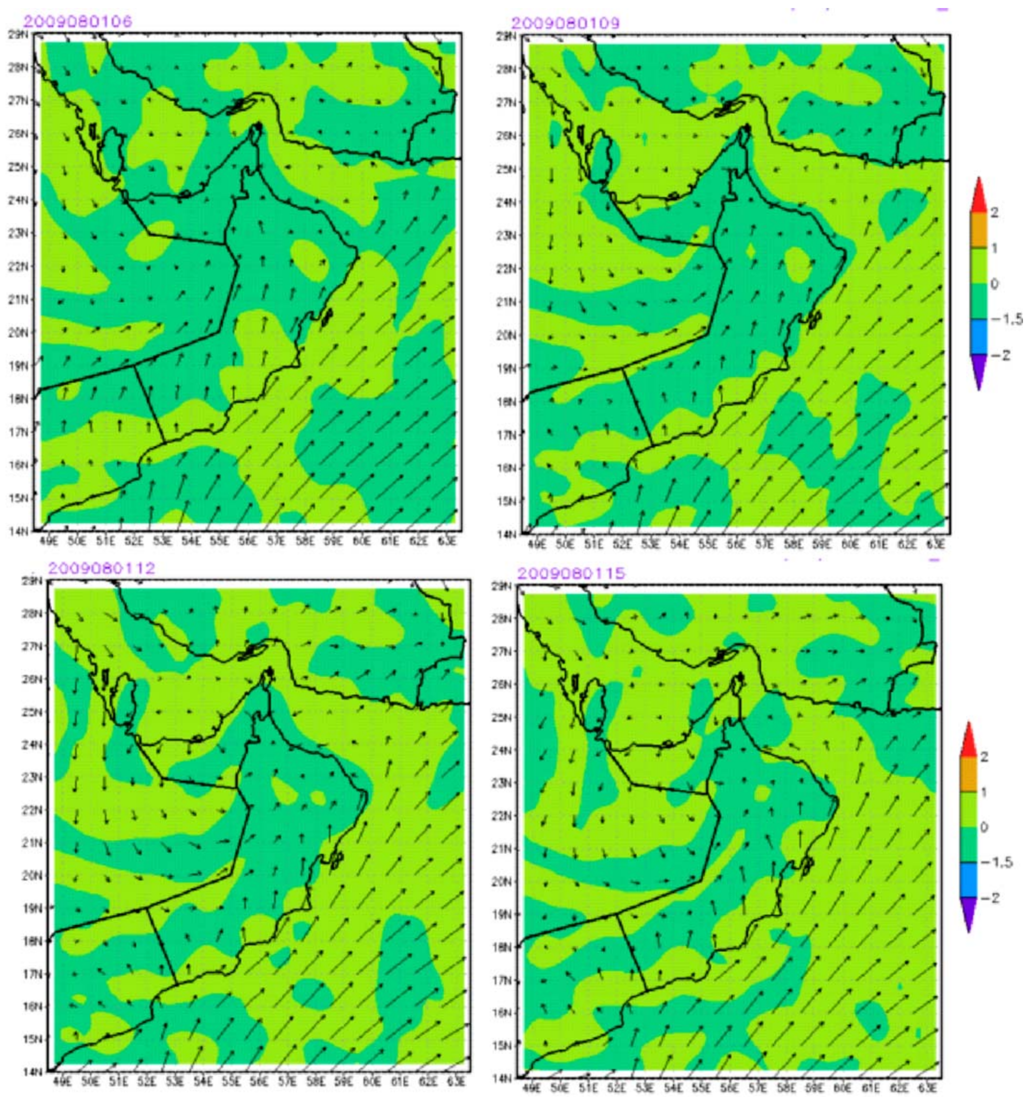


Fig. 9. HRM 28 km resolution forecast at 1000 hPa.

the lower heat capacity of Hajar mountains, strong temperature gradient is formed between sea and land which trigger the onset of sea breeze. Fig. 7 shows vertical cross section of temperature along 23.85°N (Muscat) at 8 UTC (local noon). It shows the highest temperature starts at around 58°N, which is the beginning of Hajar mountains from Muscat direction. Wind direction observations of Seeb (Muscat), Sohar and Rustaq stations are shown in Fig. 8. The red dotted line indicates the onset time (UTC) of sea breeze. It is clearly seen that sea breeze starts at one hour earlier than Sohar at about 5 UTC. It is also seen that it requires 3 h to penetrate inland until it reached Rustaq at about 8 UTC.

4. Case study results

Because of the large temperature difference between the surface temperature over land and water, sea breeze is identified by the sharp boundary, which is called sea breeze front. It is developing in the wind convergence area. Based on the conducted simulation it can be seen from Fig. 9 that the HRM forecast at 28 km resolution was not able to simulate the convergence zone (front) of the sea breeze. It was able to simulate a weak wind direction shifting over the northern coast of Oman. On the other hand, the 28 km resolution is able to simulate the south western summer monsoon. Summer monsoon is synoptic scale phenomena.

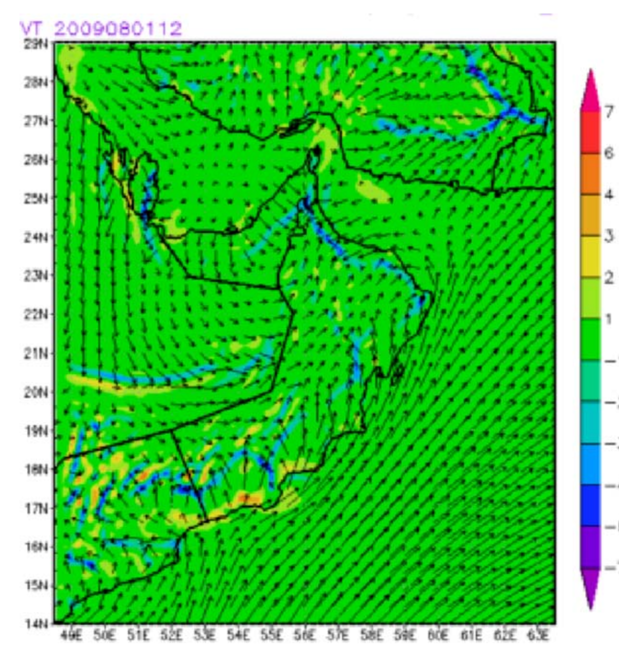


Fig. 10. HRM 7 km resolution forecast at 1000 hPa for 12 UTC.

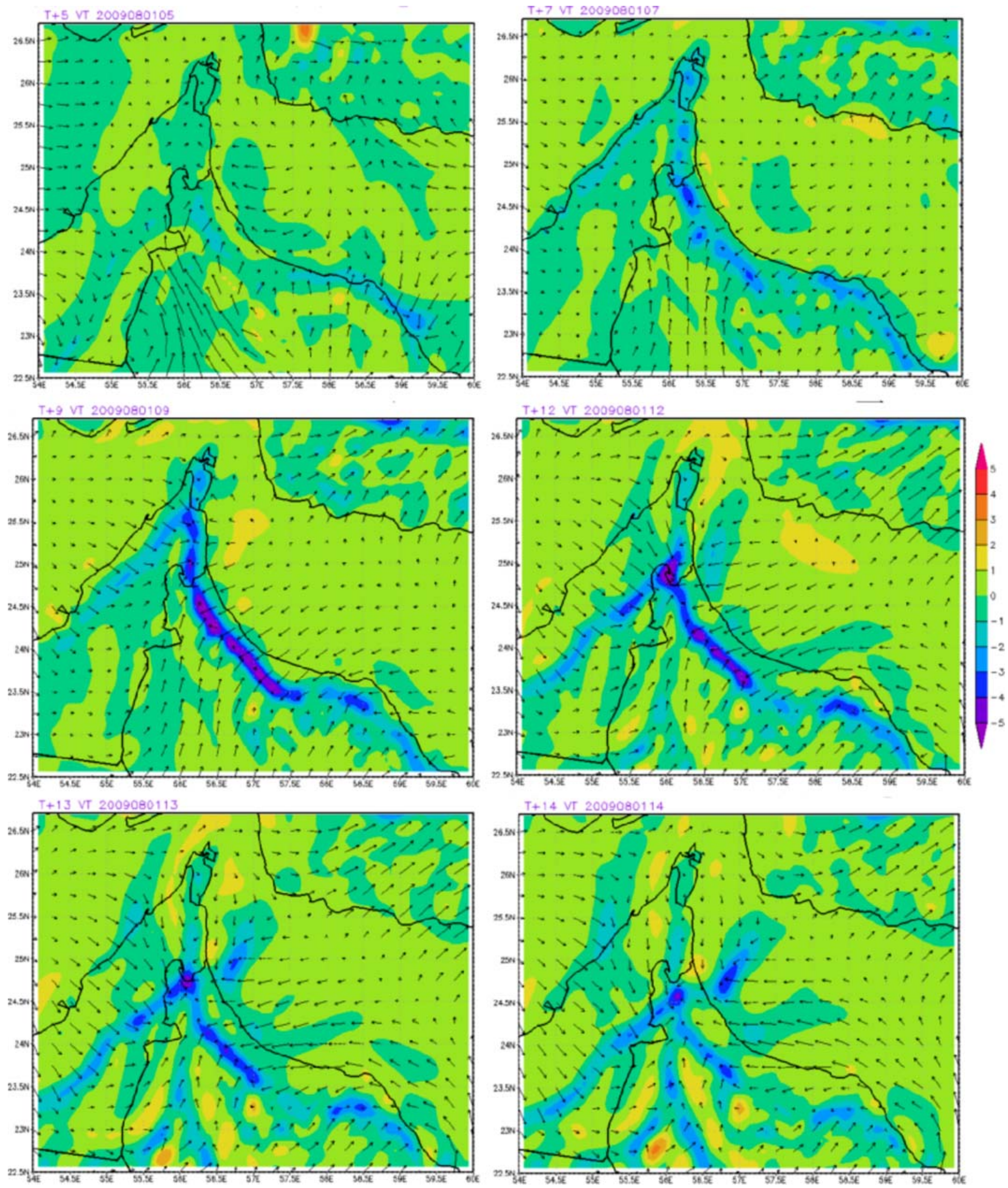


Fig. 11. Zoomed view of HRM 7 km forecast at 1000 hPa.

On the other hand, the HRM 7 km resolution forecast in Fig. 10 shows finer and smoother details of south western monsoonal flow at 1000 hPa. To identify the forecast of sea breeze front, Fig. 11 shows zoomed view over the northern coast of Oman. It clearly shows that the 7 km resolution of HRM model was able to forecast the sea breeze front to start at 5 UTC close to Muscat coast and at 7 UTC along the north coast of Oman. The onset of the sea breeze was forecasted to start at 9 UTC at the UAE side. The sea breeze front from both sides continues to penetrate inland until 14 UTC. It is clearly seen that the inland penetration of the sea breeze is blocked by the Hajar mountains in the Omani side. On the other hand, and due to the absence of the natural barrier such as mountains, sea breeze from Arabian Gulf penetrated inland much more. Calculating the distance of the perpendicular between the coast and the sea breeze front, the maximum inland penetration is around 55 km for the sea breeze coming from Oman Sea and it reached more than 180 km for the breeze coming from the Arabian Gulf. It is known that sea breeze is a shallow phenomenon, and the inland surface flow is associated with upper return current flow into the sea direc-

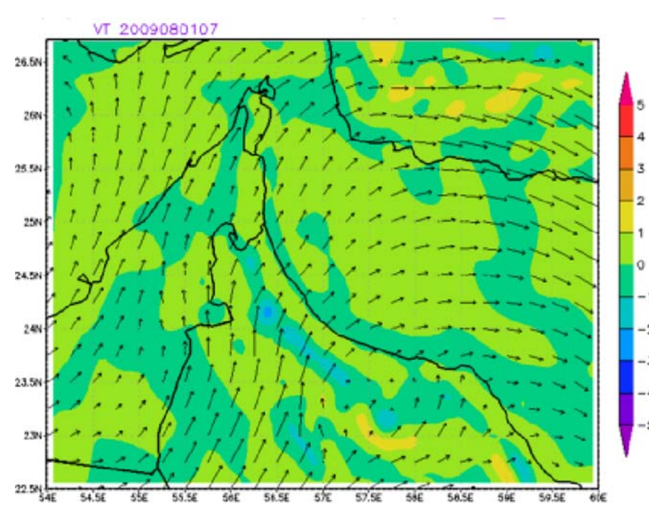


Fig. 12. HRM 7 km return current at 850 hPa.

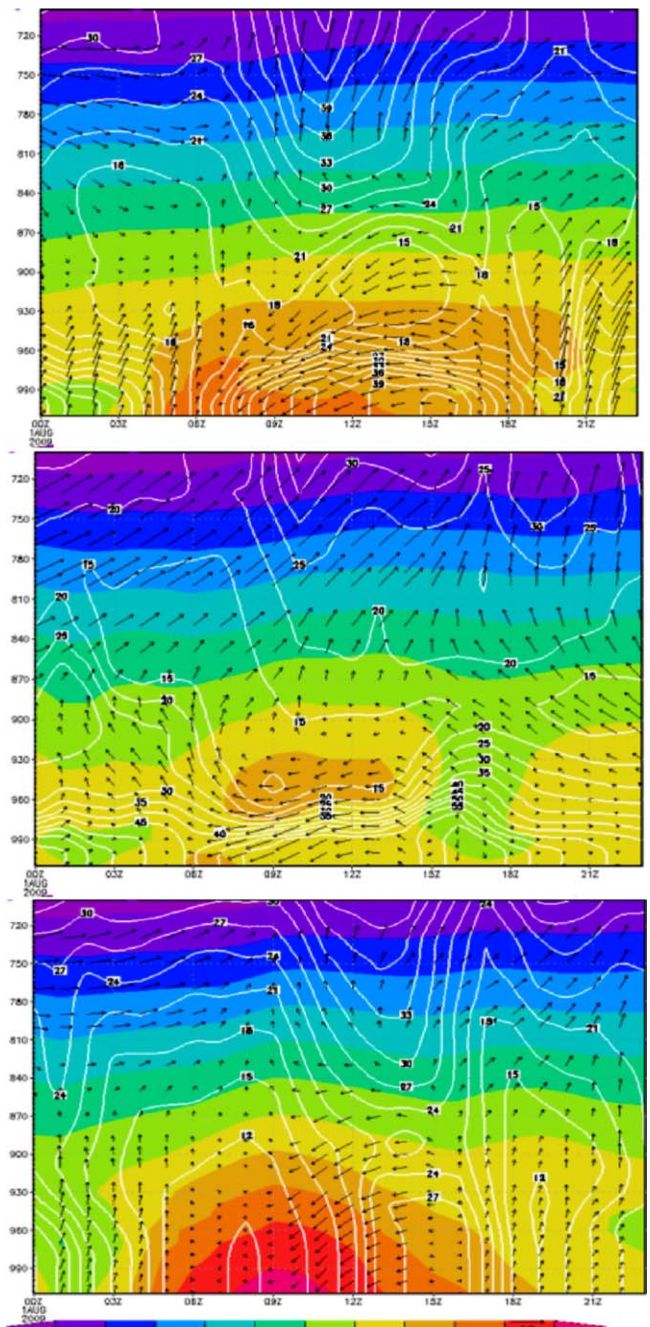


Fig. 13. HRM 7 km vertical cross-section of temperature (shaded), relative humidity (contours) and wind (arrows) for Seeb, Sohar and Rustaq.

tion. Fig. 12 shows the return current of the sea breeze forecasted by the HRM model at about 850 hPa, which is about 1.2 km above the ground.

Fig. 13 shows vertical cross section with time of HRM 7 km resolution forecast for air temperature (shaded) relative humidity (contours) and wind (arrows) at Seeb (top), Sohar (middle) and Rustaq (bottom). It shows the change of the parameters with time and altitude. North to northeasterly flow starts at 7 UTC at both Seeb and Sohar while it starts at 9 UTC at Rustaq. The forecast shows 2 h delay in the onset of the sea breeze at Seeb and 1 h delay at Sohar and Rustaq. It is clearly shown that at the onset of the sea breeze is associated with reduction in air temperature and increase of air moisture.

COSMO model also was able to forecast the sea breeze front with 7 km resolution. Fig. 14 shows zoomed view of the 1000 hPa forecast at 14 UTC. The figure shows flow and front structure similar to the structure forecasted by HRM for the same time. Vertical cross section at Sohar is shown in Fig. 15. It can be seen that COSMO model forecasted the onset of sea breeze at Sohar to start at 6 UTC, which agrees with the observation. The forecast onset of the sea breeze at Rustaq was also better than the one forecasted by HRM. The vertical cross sections also show the ability of the models to simulate the return flow of the sea breeze at about 850 hPa (∼1.3 km above the ground).

5. Wind energy assessment based on measurements, satellite, and NWP model data

At this point, it was clear that both HRM and COSMO models were able to simulate the weak local wind circulation and therefore it was decided to extend the study to evaluate the models performance for wind energy applications compared to ground measurements and satellite data. Different studies suggest that the southern part of Oman has higher potential for wind energy projects compared to the northern part of Oman. Therefore, for this part of the study, thee other stations were selected from the southern part of the country namely Qayroon Hirity, Thumrait and Masirah.

Fig. 16 shows the satellite grid box over the three stations. From the figure and due to the coarse resolution, both Thumrait and Qayroon Hirity are located in the same grid box (i.e. they have been assigned the same wind values). NWP data are based on the HRM model forecast at 7 km resolution for 2008 with 3 h intervals. The data used represents an interpolated value of the four surrounding grid point for each station. Bi-linear interpolation function has been derived and applied for the comparison. Fig. 17 shows a station (S) with the four surrounding grid points (P1–P4). Longitude and latitude are represented by λ and φ, respectively. The bi-linear interpolation function is calculated in two steps, first interpolates in the *x*-direction where $f(R_1)$, is the interpolated value at $R_1 = (\lambda_s, \varphi_i)$ and $f(R_2)$ is the interpolated value at $R_2 = (\lambda_s, \varphi_{i+1})$ as shown in the figure:

$$f(R_1) = \frac{\lambda_{i+1} - \lambda_s}{\lambda_{i+1} - \lambda i} f(P_1) + \frac{\lambda_s - \lambda_i}{\lambda_{i+1} - \lambda i} f(P_2)$$

$$f(R_2) = \frac{\lambda_{i+1} - \lambda_s}{\lambda_{i+1} - \lambda_i} f(4) + \frac{\lambda_s - \lambda_i}{\lambda_{i+1} - \lambda_i} f(3)$$

Then, interpolate in the *y*-direction, where $f(S)$ is the interpolated value at the station,

$$f(S) = \frac{\varphi_{i+1} - \varphi_s}{\varphi_{i+1} - \varphi_i} f(R_1) + \frac{\varphi_s - \varphi_i}{\varphi_{i+1} - \varphi_i} f(R_2)$$

Due to the difference in the models' resolutions, Table 1 shows the actual station elevation and the elevation seen by NWP model at 7 km and satellite model at around 111 km. Fig. 18 shows the annual (left) and summer (right) wind speed from observations, NWP, and satellite data. It can be seen that both NWP derived data and satellite data underestimate the actual wind speed. Even though the NWP wind speed forecast shows an average of about 10% underestimation for the selected stations, it shows an average of about 5% improvement over satellite data. The underestimation of wind speed is related to the difference between the actual elevation and the elevation seen by the NWP model (Table 1).

Due to the cubic relation between the wind speed and the wind power output, the 5% improvement in wind data results

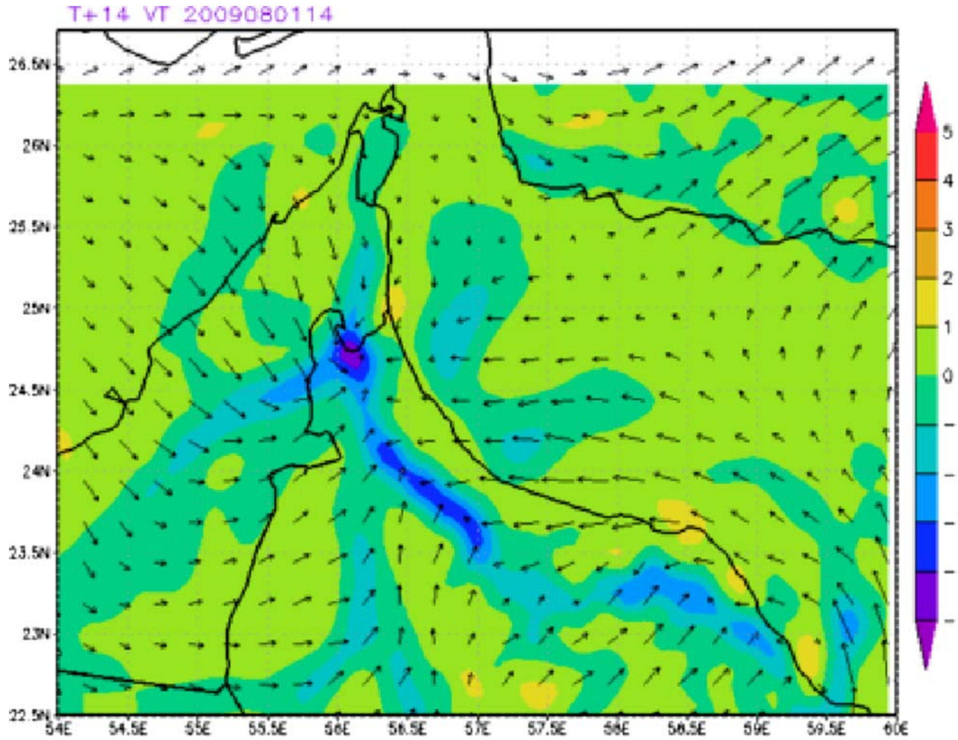


Fig. 14. Zoomed view of COSMO 7 km forecast at 1000 hPa for 14 UTC.

in an annual improvement in the wind power output from NWP data of about 19% in Qayronn Hirity, 32% in Thumrait and 34% in Masirah (Fig. 19) compared to the satellite data in the same regions.

These results clearly prove the higher accuracy of the NWP model data output compared with the satellite data output. Therefore, NWP models should be used for wind power assessment and forecasting instead satellite data which many researchers and wind power system designers are presently using in their studies. As has been shown in the previous paragraph, the errors introduced in the wind power estimation can be very high.

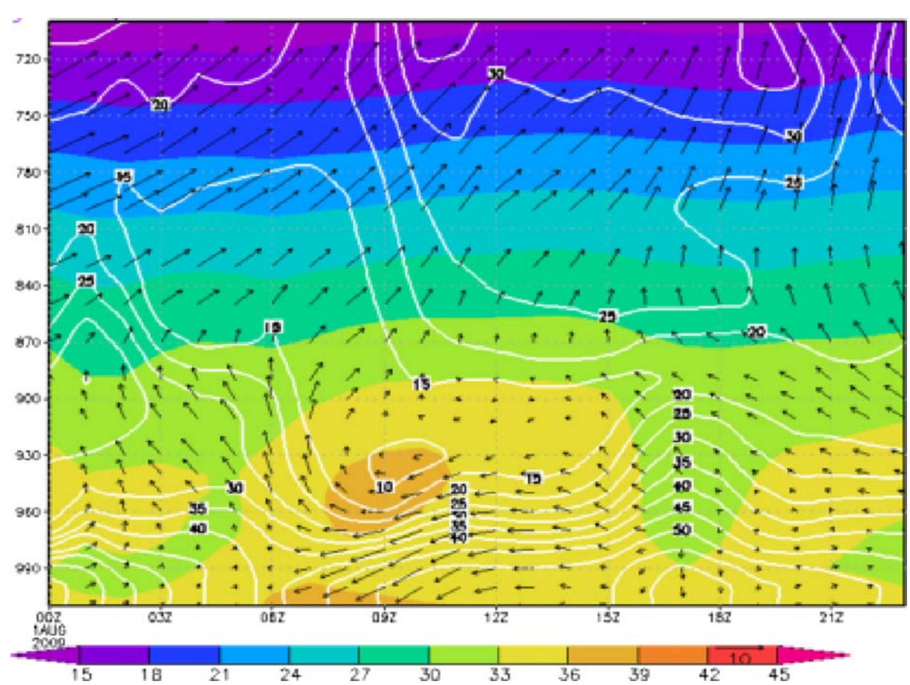


Fig. 15. COSMO 7 km vertical cross-section of temperature (shaded), relative humidity (contours) and wind (arrows) Sohar.

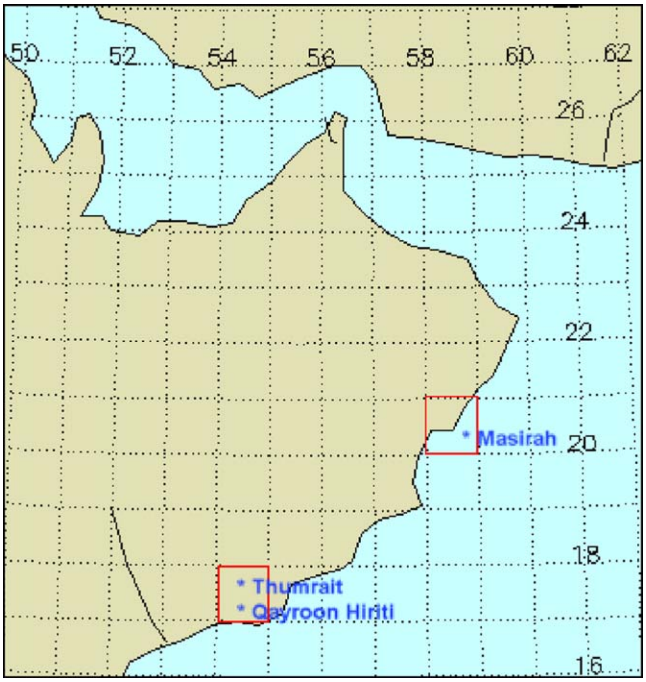


Fig. 16. Satellite grid box over Qayroon Hirity, Thumrait, and Masirah.

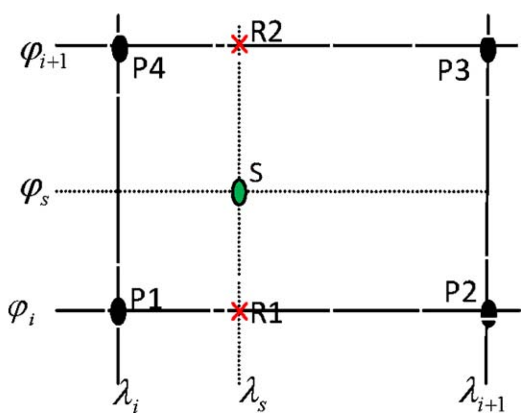


Fig. 17. Bi-linear interpolation of the four surrounding grid point of a given station S.

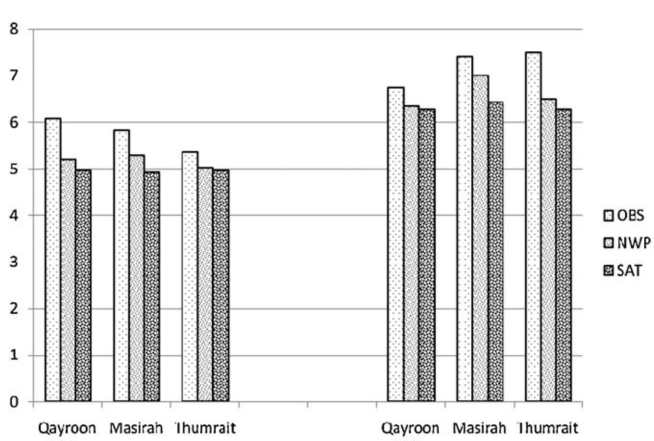


Fig. 18. Annual (left) and summer (right) wind speed (m/s).

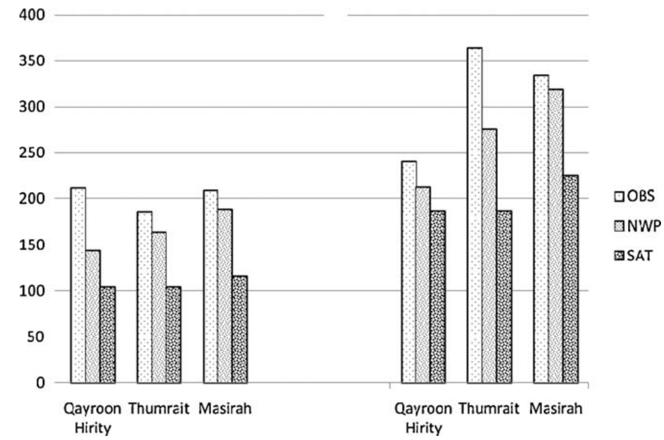


Fig. 19. Annual (Left) and summer (Right) theoretical wind power density output (W/m^2) at 10 m.

Table 1
Station elevation (m).

Qayroon hirity			Thumrait			Masirah		
Actual	NWP	SAT	Actual	NWP	SAT	Actual	NWP	SAT
878	763	547	467	436	547	19	7.8	8

6. Conclusion

The objective of this case study was to identify the ability of NWP models to simulate local sea breeze circulation. Two NWP models namely HRM and COSMO model were used with 28 and 7 km resolution. This exercise shows that 28 km resolution was not able to simulate the sea breeze front. On the other hand, both models were able to simulate the structure and the sea breeze front with good agreement with the observations using 7 km resolution. Sea breeze was found to start earlier on the Omani side than the UAE side. This is attributed to the chain of Al-Hajir mountains in the Omani side. Because mountains normally heat faster than flat land, the minimum land/sea temperature difference needed to trigger the sea breeze is reached earlier on the Omani side. It was also found that the extent of the sea breeze inland penetration is limited by the presence of Al-Hajir mountains. While the maximum inland penetration in Oman for the original field was around 55 km, the inland penetration reached 180 km in the UAE.

The first results of the wind simulation evaluation show that both HRM and COSMO models at 7 km can be used directly for local assessment of wind resources. The results obtained from the NWP were compared to actual observations and were found very accurate. However, results obtained from satellite data were not accurate and may lead to incorrect conclusions when they are used for wind power estimation and forecasting.

The improvement of the wind resource assessment passes through the improvement of spatial and temporal resolution of the NWP. In this regard, the non-hydrostatic COSMO model can be run to generate 24 h forecast at 2.2 km grid size, which is particularly suitable for complex topography. This dynamical downscaling will be useful for the wind resources assessment in Oman, since the previous studies identified an important potential of wind resources in the southern part of Oman, which is characterized by complex topography. More detailed investigations are necessary with this sub-grid model or other sub-grid scales models to evaluate their performance in air flow simulation and reducing uncertainty. Meanwhile, the effect of the smaller universal scales will be coupled with the evaluation of wind speed and power production forecasts for all sites and for different forecast ranges.

Acknowledgments

This research was funded by The Research Council (Sultanate of Oman). The authors are grateful to the Directorate General of Meteorology and Air Navigation, Sultanate of Oman for providing access to its PC Cluster to run the NWP models and providing wind hourly data for this research.

References

[1] Gastli A, Charabi Y. Solar electricity prospects in Oman using GIS-based solar radiation maps. Renewable & Sustainable Energy Reviews 2010;14(February (2)):790–7, doi:10.1016/j.rser.2009.08.018.

[2] Charabi Y, Gastli A. GIS assessment of large CSP plant in Duqum-Oman. Renewable & Sustainable Energy Reviews 2010;14(February (2)):835–41, doi:10.1016/j.rser.2009.08.019.

[3] Gastli A, Charabi Y, Zekri S. GIS-based assessment of combined CSP electric power & seawater desalinisation plant for Duqum-Oman. Renewable & Sustainable Energy Reviews 2010;14(February (2)):821–7, doi:10.1016/j.rser.2009.08.020.

[4] Merlinde JK, Nicholas C, Adam M, Lain M, Hugh O. Emerging challenges in wind energy forecasting for Australia. Australian Meteorological and Oceanographic Journal 2009;58:99–106.

[5] U.S. Department of Energy Workshop Report: Research needs for wind resource characterization. Technical report. NREL/TP-500-43521; June 2008.

[6] Al-Yahyai S, Charabi Y, Gastli A, Al-Alawi S. Assessment of wind energy potential locations in Oman using data from existing weather stations. Renewable & Sustainable Energy Reviews 2010, doi:10.1016/j.rser.2010.01.008.

[7] Pryor SC, Barthelmie RJ, Schoof JT. Inter-annual variability of wind indices across Europe. Wind Energy 2006;9:27–38.

[8] Pryor SC, Barthelmie RJ, Kjellström E. Analyses of the potential climate change impact on wind energy resources in northern Europe using output from a Regional Climate Model. Climate Dynamics 2005;25:815–35.

[9] Charabi Y, Hatrushi S. Synoptic aspects of winter rainfall variability in Oman. Atmospheric Research 2010;95(4):470–86, doi:10.1016/j.atmosres.2009.11.009.

[10] Charabi Y. Arabian summer monsoon variability: teleconexion to ENSO and IOD. Atmospheric Research 2009;91:105–17, doi:10.1016/j.atmosres.2008.07.006.

[11] Doms G., and Schattler U. A description of the Nonhydrostatic Regional Model LM. Part I: Dynamics and Numerics. Deutscher Wetterdienst (DWD), Offenbach. November 2002 [available from http://www.cosmo-model.org/content/model/documentation/core/cosmoDyncsNumcs.pdf].

[12] The Consortium for Small-scale Modeling (COSMO) (online) at www.cosmo-model.org.